JCI insight

LncRNA VINAS regulates atherosclerosis by modulating NF-κB and MAPK signaling

Viorel Simion, Haoyang Zhou, Jacob B. Pierce, Dafeng Yang, Stefan Haemmig, Yevgenia Tesmenitsky, Galina Sukhova, Peter H. Stone, Peter Libby, Mark W. Feinberg

JCI Insight. 2020. https://doi.org/10.1172/jci.insight.140627.

Research In-Press Preview Vascular biology

Graphical abstract

LncRNA VINAS regulates atherosclerosis by modulating NF-κB and MAPK signaling

Viorel Simion[1#], Haoyang Zhou[1,2#], Jacob B. Pierce[1,3], Dafeng Yang[1,2], Stefan Haemmig[1], Yevgenia Tesmenitsky[1], Galina Sukhova[1], Peter H. Stone[1], Peter Libby[1], Mark W. Feinberg[1]*

[1] Department of Medicine, Cardiovascular Division, Brigham and Women's Hospital, Harvard Medical School, Boston, MA, USA

[2] Department of Cardiology, The Third Xiangya Hospital of Central South University, Changsha, Hunan, China

[3] Feinberg School of Medicine, Northwestern University, Chicago, IL, USA

[#]Authors share equal contribution to this work.

*** Correspondence to** Mark W. Feinberg, MD, Department of Medicine, Cardiovascular Division, Brigham and Women's Hospital, Harvard Medical School, Louis Pasteur Avenue 77, 02115, Boston, Massachusetts, USA, E-mail: mfeinberg@bwh.harvard.edu, Tel: (617) 525-4381

Short title: LncRNA *VINAS* regulates vascular inflammation and atherosclerosis

Word count: 6377

Figures: 7

Supplementary Figures: 4

Key words: atherosclerosis, endothelium, lncRNA, vascular inflammation

Conflict of interest statement: The authors have declared that no conflict of interest exists.

Non-standard Abbreviations and Acronyms

VINAS	**V**ascular **IN**fllammation and **A**therosclerosis lncRNA **S**equence
DEPDC4	DEP (Dishevelled, Egl-10 and Pleckstrin) Domain Containing 4
BMDM	Bone marrow derived macrophages
CPM	Counts per million
CVD	Cardiovascular disease
EC	Endothelial cell
HCD	High cholesterol diet
IHC	Immunohistochemistry
lncRNA	long non-coding RNA
MAPK	Mitogen-activated protein kinases
NF-κB	nuclear factor kappa-light-chain-enhancer of activated B cells
NOR	No overlapping reads
PBMC	Peripheral blood mononuclear cell
RT-qPCR	Real-time polymerase chain reaction
TNFα	Tumor necrosis factor alpha
VCAM-1	Vascular cell adhesion molecule
ICAM-1	Intracellular adhesion molecule
IL-1β.	Interleukin beta
COX-2	Cyclooxygenase
MCP-1	Monocyte Chemoattractant Protein-1

Abstract

Long non-coding RNAs (lncRNAs) play important roles in regulating diverse cellular processes in the vessel wall, including atherosclerosis. RNAseq profiling of intimal lesions revealed a lncRNA, ***VINAS*** (**V**ascular **IN**fllammation and **A**therosclerosis lncRNA **S**equence), that is enriched in the aortic intima and regulates vascular inflammation. Aortic intimal expression of *VINAS* fell with atherosclerotic progression and rose with regression. *VINAS* knockdown reduced atherosclerotic lesion formation by 55% in LDLR-/- mice, independent of effects on circulating lipids, by decreasing inflammation in the vessel wall. Loss- and gain-of-function studies *in vitro* demonstrated that *VINAS* serves as a critical regulator of inflammation by modulating NF-κB and MAPK signaling pathways. *VINAS* knockdown decreased the expression of key inflammatory markers, such as MCP-1, TNF-α, IL-1β , COX-2, in endothelial (EC), vascular smooth muscle cells, and bone marrow-derived macrophages. Moreover, *VINAS* silencing decreased expression of leukocyte adhesion molecules VCAM-1, E-selectin, and ICAM-1 and reduced monocyte adhesion to ECs. DEPDC4, an evolutionary conserved human ortholog of *VINAS* with ~74% homology, shows similar regulation in human and pig atherosclerotic specimens. DEPDC4 knockdown replicated *VINAS*' anti-inflammatory effects in human ECs. These findings reveal a novel lncRNA that regulates vascular inflammation, with broad implications for vascular diseases.

Introduction

Accumulating studies highlight that inflammatory processes and traditional cardiac risk factors may cooperatively contribute to vascular disease leading to the development of cardiovascular events (1) (2). Although Virchow hypothesized involvement of inflammation in atherosclerosis over 150 years ago (3), only recently did the CANTOS trial confirm in humans the inflammatory hypothesis of atherosclerosis, by showing that neutralization of the pro-inflammatory cytokine IL-1β reduced recurrent cardiovascular events independent of changes in serum lipid levels (4) (5).

Inflammation impairs endothelial functions. For example, in response to both biochemical (e.g. IL-1β, modified-LDL) and biomechanical (e.g. disturbed blood flow) stimuli, endothelial activation occurs early in atherogenesis (6). Expression of adhesion molecules (e.g. VCAM-1, E-Selectin, ICAM-1) and secretion of chemokines (e.g. MCP-1) facilitates the recruitment of leukocyte subsets into the vessel wall (7). Impaired endothelial barrier function accompanies vascular inflammation and atherosclerosis (1) (8). Similar to ECs, SMCs can also express a variety of adhesion molecules in response to cytokine stimulation to which monocytes and lymphocytes can adhere and migrate into the vessel wall (9) (10) (5). However, major mechanistic gaps remain in our understanding of regulatory pathways involved in homeostasis of the vessel wall in response to pathophysiological stimuli, contributing to the dearth of targeted therapeutics in a range of vascular disease states.

Recently, lncRNAs have emerged as powerful regulators of nearly all biological processes by exerting epigenetic, transcriptional, or translational control of target genes due to their polyvalent binding properties to RNA, DNA, and protein as well as acting as molecular sponges for other transcripts and miRNAs (11) (12). However, the role of lncRNAs in vascular inflammation and cardiovascular diseases (CVD) is only emerging (13). Identification of lncRNAs specifically expressed in the vascular intima of lesions during the progression of atherosclerosis may provide insight into their roles in atherogenesis and potentially uncover new insights for vascular inflammation in advanced lesions (14).

This study identifies the lncRNA *VINAS* as a key regulator of vascular inflammation and atherosclerotic lesion formation. We further find that its human ortholog DEPDC4 is similarly expressed in atherosclerotic lesions and phenocopied effects on human endothelial cell

inflammation. Collectively, these findings provide new insights for lncRNA-mediated control of inflammation in the vessel wall.

Results

Identification and characterization of *VINAS* lncRNA

LDLR$^{-/-}$ male mice were placed on a high cholesterol diet (HCD) for 0, 2, and 12 weeks (progression phases; groups 1-3) and subsequently placed on chow diet for another 6 weeks in the fourth group (regression phase, Fig. 1A). RNA was isolated from the aortic intima and RNA-Seq profiling revealed 11 differentially expressed lncRNAs (log2-fold change (1.5); FDR<0.05) using EdgeR and NOR (No Overlapping Reads) algorithms (Fig. 1B). 8 lncRNAs rose with atherosclerosis progression (group 3) and fell during regression (group 4), while only 3 lncRNAs were decreased with atherosclerosis progression (Fig. 1C). The lncRNA 1500026H17Rik showed the strongest decrease in group 3 (by 59%), while regaining initial levels with atherosclerosis regression as quantified by RT-qPCR (Fig. 1C, D). Because of its high regulability and participation in both vascular inflammation and atherosclerosis, as we show here, we have named this lncRNA ***VINAS*** (**V**ascular **IN**fllammation and **A**therosclerosis lncRNA **S**equence).

Further experiments characterized arterial *VINAS* expression. *VINAS* expression is higher in endothelial cells (ECs isolated from lungs and Bend.3 cell line) compared to other cell types such as vascular smooth muscle cells (MOVAS cell line), NHI3T3 fibroblasts, bone marrow-derived macrophages or the RAW 264.7 macrophage cell line (Fig. 1E), and is broadly expressed in several other organs, with a strong enrichment in the aortic intima compared to the media in the vessel wall (Fig. 1F). Our previous study verified the specificity of aortic intima isolation (15) To test whether *VINAS* lncRNA indeed does not encode a protein or peptide, the *VINAS* sequence was cloned upstream of the p3xFLAG-CMV plasmid, transfected in HEK293 cells, and immunoblotted for FLAG Tag, yielding no detectable peptide or protein (Fig. 1G). Additionally, *VINAS* was found to be polyadenylated (Fig. 1H) and is enriched in the cytosol as observed by cellular fractionation and by RNA-ISH in mouse ECs (Fig. 1I, J).

VINAS regulates inflammation in vascular cells

ECs participate pivotally in vascular inflammation and development of atherosclerosis. Because *VINAS* is enriched in ECs (Fig.1E) the potential phenotype of *VINAS* loss- and gain-of-function was assessed in mouse ECs. For the knockdown strategy, we designed 3 different locked nucleic acid (LNA)-gapmeRs (Suppl. Fig. 1B). GapmeR #2 showed the highest silencing efficiency in a dose-dependent manner (Suppl. Fig. 1C) and it was used throughout the study. The gapmeR-mediated knockdown of *VINAS* dramatically decreased the mRNA expression of the adhesion molecules VCAM-1 by ≈ 50-95% and E-selectin by ≈ 40-65% in ECs activated with 0.5, 1, and 2.5 ng/ml of TNF-α or IL-1β (Fig. 2A-B). In addition, *VINAS* knockdown in activated ECs reduced the mRNA expression of the chemokine MCP-1, by ≈ 50-80% and the inflammatory molecule COX-2 by ≈ 40-55% (Fig. 2A-B). Moreover, *VINAS* silencing produced similar effects at the protein level, decreasing VCAM-1 by ≈ 45-55% after activation with 20 ng/ml TNF-α or IL-1β (Fig. 2C, D), and MCP-1, COX-2, and IL-1β by ≈ 50% (Fig. 2E-G). Transfection with 2 different *VINAS* gapmeRs (gapmeR #1 and #3) produced comparable decreases in VCAM-1 and COX-2 in ECs activated with 20 ng/ml TNF-α (Supplementary Figure 1E). In contrast, overexpression of *VINAS* using a pCDNA3 plasmid (Supplementary Figure 1D) had the opposite effect in mouse ECs, increasing the protein expression of VCAM-1 (20%), ICAM-1 (26%) and IL-1β (35%) (Fig. 2H-J). Because *VINAS* knockdown in ECs decreased the expression of VCAM-1 and E-selectin, two cell adhesion molecules known to mediate leukocyte adhesion to ECs, we assessed adhesion of peripheral blood mononuclear cells (PBMCs) to EC monolayers in response to 10 ng/ml of TNF-α stimuli. *VINAS* knockdown reduced PBMCs adherence to EC monolayers by 29% ($p<0.0001$), verifying the functional importance of *VINAS* lncRNA in leukocyte-EC cellular interactions (Fig. 2K). Further experiments assessed the anti-inflammatory actions of *VINAS* in two other cell types that are enriched in atheroma: vascular smooth muscle cells and bone marrow-derived macrophages. We observed similar effects of *VINAS* knockdown in the MOVAS smooth muscle cell line with reduced expression of VCAM-1 (70%), ICAM-1 (40%), and MCP-1 (22%) at the mRNA level (Fig. 3A-C) and decreased protein expression of VCAM-1 (34%), ICAM-1 (72%), MCP-1 (22%), TNF-α (37%) and IL-1β (44%) after stimulation with 5 ng/ml of TNF-α (Fig. 3D-H). Consistently, *VINAS* silencing also decreased COX-2 (19%), IL-1β (38%), and MCP-1 (37%) in primary bone marrow-derived macrophages

stimulated with 50 ng/ml LPS (Fig. 3K). Collectively, these findings indicate that *VINAS* broadly regulates inflammatory mediators in relevant cell types in the vessel wall. The stronger anti-inflammatory phenotype observed in endothelial cells compared to VSMCs and BMDMs correlates with the increased expression of *VINAS* in ECs (Fig. 1E).

VINAS regulates NF-κB and MAPK signaling pathways in endothelial cells

To identify potential signaling pathways subject to *VINAS* regulation, ECs transfected with *VINAS* gapmeRs were activated with 20 ng/ml TNF-α for 5 to 60 minutes and assessed for expression of key pro-inflammatory signaling pathways. Immunoblotting showed that *VINAS* knockdown significantly decreased the phosphorylation of IκB-α in ECs activated with TNF-α (20 ng/ml) by 35%, 33% and 37% after 5, 15 and 30 minutes respectively (Fig. 4A). In addition, silencing of *VINAS* in ECs reduced the phosphorylation of p38 MAPK by 55-75% in the presence of TNF-α (20 ng/ml) for 15, 30 and 45 minutes (Fig. 4B). Similar conditions were tested for AKT signaling pathway and showed no specific effect of *VINAS* silencing on AKT phosphorylation (Fig. 4C). Taken together, these findings indicate that *VINAS* knockdown regulates predominantly the NF-kB and MAPK signaling pathways.

In vivo knockdown of *VINAS* markedly reduced atherosclerotic lesion formation by decreasing vascular inflammation

To explore whether systemically delivered *VINAS*-gapmeRs modulates atherosclerosis, LDLR-/- mice received i.v. injections of vehicle control or *VINAS*-gapmeR (10 mg/kg/2x weekly) over 12 weeks on a high cholesterol diet (HCD) (Fig. 5A). After 12 weeks on HCD, gapmeR-mediated silencing of *VINAS* reduced its expression in the aortic intima by 57% (Fig. 5H) and in the media by 30% (Fig. 5I),

Analysis of atherosclerotic lesion formation by Oil-Red O (ORO) staining revealed a 55% decrease in lesion area in the aortic sinus after antagonism of *VINAS* (Fig. 5B). While *VINAS* knockdown was associated with a modest reduction in total cholesterol (22%), LDL (25%), HDL (6%) and triglycerides (7%) (Supplementary Fig. 2A), the lesion areas as quantified

by Oil Red O staining remained 48% smaller in *VINAS* knockdown mice when examined in mice with similar total cholesterol in both groups (Supplementary Fig. 2B). Although ~8% of the atherosclerotic plaque reduction may be accounted for effects on cholesterol metabolism, it cannot account entirely for the marked reduction in atherosclerosis lesions following *VINAS* knockdown.

Immunohistochemistry (IHC) staining revealed that VCAM-1 and the macrophage marker Mac-2 decreased by 38%, and 43%, respectively, in the aortic sinus indicating reduced vascular inflammation and macrophage accumulation in the vascular wall (Fig. 5C and 5D). No significant differences were observed for CD4+ or CD8+ T cells or vascular smooth muscle cells after normalization to lesion area (Fig. 5E-G). *In vivo* knockdown of *VINAS* in the aortic intima reduced the expression of inflammatory markers TNF-α, MCP-1, ICAM-1, COX-2, and IL-1β (Fig. 5H). Moreover, *VINAS* knockdown in the aortic media decreased inflammatory effectors such as COX-2, IL-1β, E-selectin, VCAM-1, and ICAM-1 (Fig. 5I). While *VINAS* silencing also reduced circulating PBMCs (62%), it did not significantly alter mRNAs that encode the inflammatory mediators TNF-α, IL-1β, COX-2 and MCP-1 in these cells (Suppl. Fig. 1F). Nor did *VINAS*-knockdown alter the anti-inflammatory $Ly6C^{low}$ or the pro-inflammatory $Ly6C^{interm}$ or $Ly6C^{high}$ fractions in the PBMCs as determined by flow cytometry (Suppl. Fig. 1G). Overall, *VINAS* neutralization in $LDLR^{-/-}$ mice fed HCD for 12 weeks muted atherosclerotic lesion formation in tandem with decreased inflammation.

DEPDC4 is a *VINAS* ortholog conserved in humans

While *VINAS* lncRNA is only present in the mouse genome, we observed that the genomic locus is largely conserved, with the genes SCYL2, ACTR6 and ANKS1B in the immediate proximity and the gene DEPDC4 (DEP Domain Containing 4) in the same position as *VINAS* (Fig. 6A). BLAST findings showed that DEPDC4 has a ~74% homology with *VINAS* in a region of 157-323 bp, depending on isoform variations (Suppl. Fig. 4A). DEPDC4 is widely conserved across species, except for the mouse (Suppl. Fig. 4A). To verify the coding probability, the DEPDC4 sequence was cloned upstream of the p3xFLAG-CMV plasmid, transfected in HEK293 cells, and immunoblotted for FLAG Tag. The resulting immunoblot

showed no detectable peptide or protein (Fig. 6B). As with *VINAS* loss of function in mouse cells, DEPDC4 knockdown (Supplementary Fig. 4B) induced an anti-inflammatory program in HUVECs stimulated with TNF-α, decreasing the expression of VCAM-1 (42%), E-selectin (40%), and COX-2 (30%) (Fig. 6C-E). We then assessed adhesion of THP-1 monocytes to a monolayer of HUVECs in response to TNF-α stimulation. DEPDC4 silencing significantly decreased monocyte adherence to the EC monolayer by 30%, verifying the functional importance of DEPDC4 lncRNA in leukocyte-EC cellular interactions (Fig. 6F).

To assess the translational relevance of *VINAS* and DEPDC4 lncRNAs, RNA was isolated from human carotid atherosclerotic plaques with characteristics associated with stability or instability. The expression of DEPDC4 is decreased by 77.4% in carotid arteries with plaques with unstable vs. those with stable features (Fig. 6G). To explore this expression pattern across species, we analyzed the RNA-Seq data from Yorkshire pigs that were placed for up to 60 weeks on an HCD and developed coronary atherosclerosis. Based on histopathological characterization, the coronary sections were separated into mild, intermediate, and severe groups for progression of atherosclerosis as described elsewhere (15). Similar to *VINAS* regulation in LDLR-/- mice fed HCD (Fig. 1C), DEPDC4 was decreased ~60% with disease progression in swine pigs fed HCD (Fig. 6H). Concordantly, in endothelial cells stimulated with TNF-α expression of *VINAS* and DEPDC4 also decrease after 4-8 hours and 16-24 hours, respectively (Suppl. Fig 1H, I). In summary (Fig. 7), these results demonstrate dynamic regulation of the lncRNA *VINAS* with atherosclerosis progression, *VINAS* influences arterial inflammation, and that loss of function of *VINAS*' evolutionary conserved lncRNA ortholog DEPDC4 exerts similar anti-inflammatory effects.

Discussion

Arterial inflammation occurs very early in atherogenesis and is associated with impairment of many salutary functions of the healthy endothelium. Accumulating studies point to lncRNAs as regulators of endothelial homeostasis, smooth muscle cell contractility, and macrophage-mediated inflammation in the vessel wall (11) (13) (15) (16) (17) (18). This study

provides evidence for the first time that the mouse-specific lncRNA *VINAS* and its human ortholog DEPDC4 play important roles in vascular inflammation and atherogenesis.

Our study expands upon a growing body of literature implicating lncRNAs as pivotal regulators in the development and progression of atherosclerosis. Our group recently identified SNHG12 as an evolutionarily conserved lncRNA that plays an important role in atherogenesis (15). SNHG12 mediated the interaction between DNA damage repair proteins DNA-PK and its binding partners Ku70 and Ku80. Following *SNHG12* knockdown in $LDLR^{-/-}$ mice, atherosclerotic lesion area increased by 240% with corresponding increases in markers of DNA damage and endothelial cell senescence (15). The lncRNAs *LeXis* and *MeXis* were identified as key regulators of cholesterol metabolism (19, 20). Both of these lncRNAs are transcriptionally regulated by the liver X receptor, a nuclear sterol receptor responsible for transcriptional control of genes involved with cholesterol metabolism. *LeXis* interacted with the ribonuclear protein RALY to aid in transcription of cholesterol metabolism genes in the liver, and *in vivo* delivery of *LeXis* using an adenoviral vector reduced aortic atherosclerosis in mice (21). *MeXis* altered expression of *ABCA1* via its binding partner DDX17, and genetic abrogation of *MeXis* increased serum cholesterol and atherosclerotic lesion area (20).

Similar to *VINAS*, a few other lncRNAs regulate atherosclerosis by modulating inflammatory pathways. For example, the lncRNA *NEXN-AS1* lies antisense to and increases the expression of NEXN, a protein that negatively regulates TLR4 and NF-κB signaling (22). Genetic depletion of *NEXN-AS1* dramatically increased atherosclerosis in $ApoE^{-/-}$ mice with concurrent increases in markers of vascular inflammation such as VCAM1, ICAM1, TNF-α, and MCP-1. Similarly, knockdown of *lncRNA-FA2H-2* increased atherosclerotic plaque size and expression of inflammatory genes. Here, we show that *VINAS* plays an analogous role in inflammation and atherogenesis, albeit as a pro-inflammatory lncRNA in contrast to the anti-inflammatory lncRNAs *NEXN-AS1* or *lncRNA-FA2H-2*. *In vivo* delivery of *VINAS*-specific LNA gapmeRs significantly decreased the expression of important inflammatory mediators and cell adhesion molecules in the intima as well as the media of the aortic arch. *VINAS* silencing exerted strong anti-inflammatory effects across different cellular constituents of the vessel wall, demonstrated by decreased key inflammatory effectors such as MCP-1, TNF-α, IL-1β, COX-2, and the leukocyte adhesion molecules VCAM-1, E-selectin, or ICAM-1 in both endothelial and

vascular smooth muscle cells (Fig. 2, 3). The stronger anti-inflammatory phenotype observed in in ECs and the intima is likely due to increased *VINAS* silencing efficiency (Fig. 5H, I and Supplementary Fig. 1B, C) coupled with the relatively higher expression of VINAS in ECs and intima (Fig. 1E, F) compared to the aortic media. Also, the aortic media is composed of more heterogeneity of cell types (e.g. fibroblasts, VSMCs, immune cells) and *VINAS* expression is variable across these different cell types (Fig. 1E).

Leukocyte adhesion to activated ECs overexpressing adhesion molecules such as VCAM-1 and E-selectin is amongst the earliest processes involved in atherosclerotic lesion initiation (23) (24). This study shows that *VINAS* knockdown in TNF-α-activated ECs significantly reduced monocyte adhesion to EC monolayers (Fig. 2K). In line with this finding, *in vivo VINAS* knockdown decreased the staining of macrophage marker Mac-2 in the aortic root, suggesting a diminished macrophage accumulation in the vessel wall due to lower expression of cell adhesion molecules (Fig. 5D). Macrophage polarization to a pro-inflammatory phenotype contributes to the progression and destabilization of atherosclerotic plaques. For example, symptomatic patients suffering from acute transient ischemic attacks with unstable plaques had a higher concentration of M1 pro-inflammatory macrophages in lesions compared to asymptomatic patients with stable plaques (25) (26). Although the M1/M2 macrophage dichotomy oversimplifies macrophage heterogeneity, an M1 pro-inflammatory macrophage predominance in atherosclerotic plaques associates with a higher incidence of ischemic stroke and increased lesional inflammation (27). Moreover, plaques from patients with recently symptomatic carotid disease have a predominance of M1-macrophages and higher lipid content than femoral plaques, consistent with a more unstable plaque (28). While *VINAS* knockdown in bone marrow-derived macrophages *in vitro* decreased the expression of MCP-1, IL-1β, and COX-2, (Fig. 3K), there were no differences in these effectors or of Ly6C+ pro-inflammatory in PBMCs *in vivo,* suggesting that the anti-inflammatory effects of *VINAS* knockdown *in vivo* were likely driven more by impacting leukocyte adhesion molecules in intimal ECs (Figs 2,3). While the dominant impact of lncRNA VINAS knockdown is regulating inflammation in the vessel wall with a 48% reduction in atherosclerotic plaque when cholesterol values are normalized between the groups (Supplementary Fig. 2B), we cannot exclude a minor contribution to cholesterol metabolism.

Identification of the potential signaling pathways that lncRNAs regulate is critical from a therapeutic point of view. In some cases, deciphering the signaling pathway and its upstream or downstream regulators can indicate the mechanisms used by a specific lncRNA (29). In this study, *VINAS* and DEPDC4 knockdown in cytokine-activated ECs reduced the phosphorylation of IKB-α and p38 MAPK while having no significant effects on phosphorylation of AKT signaling pathway (Fig. 4). Both the NF-κB and p38 MAPK inflammatory pathways serve as critical nodal points of regulation in atherosclerosis, particularly in the vascular endothelium (30-32). Gareus et al. demonstrated that endothelial-specific genetic depletion of IKKγ or IκBα, key signaling molecules in the NF-κB pathway, was sufficient to significantly reduce atherosclerosis in *ApoE*$^{-/-}$ mice (33). Systemic delivery of microRNAs that inhibit NF-κB activation in the vascular endothelium also reduced inflammation and atherosclerosis lesion in *ApoE*$^{-/-}$ mice (34). Similarly, p38 MAPK inhibitors decreased levels of systemic and vascular inflammation in both mouse models of atherosclerosis (35, 36) as well as humans with coronary artery disease (37, 38). Furthermore, Seeger et al. demonstrated that systemic p38 MAPK inhibition for four weeks reduced atherosclerotic lesion size by more than 50 percent (36). Our study extends these findings by showing that lncRNA *VINAS* is an important regulator of NF-κB and p38 MAPK signaling pathways and thus exerts considerable control over the development of vascular inflammation and atherosclerosis. The observed anti-inflammatory phenotype induced by *VINAS* knockdown may inform the potential upstream mechanisms by which this lncRNA impacts these inflammatory pathways. *VINAS* lncRNA is enriched in the cytosol and its knockdown potently reduced the phosphorylation of p38 MAPK, a signaling pathway with its main effectors localized in the cytosol (39) (40) (41) (42) (43). While cytosolic lncRNAs have been reported to interact with miRNAs by a base pair binding mechanism (44) (45), this competing endogenous RNA (ceRNA) hypothesis remains controversial in the field. An *in vivo* quantitative study showed that modulation of a miRNA target abundance is unlikely to cause significant effects on gene expression and metabolism through a ceRNA effect (46). Future studies exploring the candidate factor(s) mediating this inhibition of dual signaling pathways may further elucidate potential therapeutic targets for atherosclerosis and other chronic inflammatory disease states.

Finally, while lncRNAs are not typically as conserved across species compared to other non-coding RNAs, such as microRNAs, emerging studies demonstrate conservation via

orthologous transcripts (20). Finding an evolutionary conserved transcript DEPDC4, a human ortholog of *VINAS* in humans with ~74% homology, exhibit regulation in human EC cells congruent to the effects of *VINAS* on mouse cells supports the human relevance of the present mouse findings. Consistent with *VINAS* regulation in atherosclerotic mice, DEPDC4 levels decline in coronary arteries of pigs with progression of atherosclerosis and in human carotid plaques with unstable characteristics (Fig. 6G-I). *VINAS* expression also decreases in ECs after 4- and 8-hours incubation with TNF-α, while returning to basal levels after 16 to 24 hours (Suppl. Fig 1H). In all our experiments the cytokines were added to the cells at 48 hours after gapmeRs transfection, when the *VINAS* silencing efficiency was already achieved by ~90%. Hence, the potential *VINAS* downregulation after cytokines addition would be negligible. Several mechanisms can be responsible for the observed *VINAS* regulation, including compensatory or feedback mechanisms in response to stress induced by inflammatory stimuli. For instance, LPS induces inflammation via the NF-κB pathway. However, LPS also induces the synthesis of anti-inflammatory cytokines such as IL-10 and IL-4, which in turn blocks NF-κB activation in a negative feedback mechanism (47) (48), suggesting that the upregulation of anti-inflammatory genes are not always coincident with inflammatory state. Indeed, lncRNAs can be regulated as a negative feedback during inflammation. For example, LPS increases the expression of lncRNA Mirt2. However, lncRNA Mirt2 serves as a negative feedback regulator of excessive inflammation and reduces inflammation across different cell types (49). Interestingly, the IL-10 anti-inflammatory phenotype is regulated by the ubiquitously expressed transcription factor Sp1 (50), which also has multiple binding sites in the *VINAS* and DEPDC4 promoters (Supplementary Table 2). While we have not identified the exact mechanism for the upstream regulation of *VINAS* lncRNA, we cannot rule out the existence of a compensatory mechanism in response to pro-inflammatory stimuli. Future studies will need to assess the specific upstream mechanism of *VINAS* / DEPDC4 regulation at the promoter and the transcript levels and whether this is a regulatory effect on RNA stability or a compensatory mechanism in the cell.

In conclusion, the discovery of *VINAS* reported here extends the understanding of participation of lncRNAs in inflammatory signaling in general and in the pathogenesis of atherosclerosis and potentially other vascular diseases as well. Modulation of lncRNAs *VINAS* and DEPDC4 may facilitate “fine-tuning” of the inflammatory response in a range of chronic vascular diseases, and perhaps of other organ systems as well.

369

370

371

372

Materials and methods

RNA-Seq Analysis

RNA-Seq analysis was performed after ribodepletion and standard library construction using Illumina HiSeq2500 V4 2x100 PE (Genewiz, South Plainfield, NJ). All samples were processed using an RNA-seq pipeline implemented in the bcbio-nextgen project (https://bcbio-nextgen.readthedocs.org/en/latest/). Raw reads were examined for quality issues using FastQC (http://www.bioinformatics.babraham.ac.uk/projects/fastqc/) to ensure library generation and sequencing were suitable for further analysis. Trimmed reads were aligned to UCSC build mm10 of the Mouse genome, augmented with transcript information from Ensembl release 79 using STAR (51). Alignments were checked for evenness of coverage, rRNA content, genomic context of alignments (for example, alignments in known transcripts and introns), complexity and other quality checks using a combination of FastQC, Qualimap. Counts of reads aligning to known genes were generated by featureCounts (52). Differential expression at the gene level were called with EdgeR. The total gene hit counts and CPM values were calculated for each gene and for downstream differential expression analysis between specified groups was performed using EdgeR and an adapted EdgeR algorithm, which excludes overlapping reads, called no-overlapping reads (NOR). Genes with adjusted FDR< 0.05 and log2fold-change (1.5) were called as differentially expressed genes for each comparison. Mean quality score of all samples was 35.67 within a range of 40,000,000-50,000,000 reads per sample. All samples had at least >70% of mapped fragments over total.

Polyadenylation

RNA of 10^6 ECs was isolated using TRIzol reagent (Invitrogen) and resuspended in RNase-free water. Polyadenylated and non-polyadenylated RNA was enriched with polyA Spin mRNA isolation kit (NEB, S1560S) based on manufacturer's protocol. RT-PCR was performed with same input volume, independent of concentration and normalized to non-polyadenylated RNA fraction.

RNA-ISH

Customized probe for *VINAS* was specifically developed to detect ENSMUST00000181598 (Advanced Cell Diagnostics). BMDMs were fixed in 4% paraformaldehyde and the *in situ*

hybridization protocol for cultured adherent cells was performed as described by the manufacturer (Basescope 2.5 HD Reagent Kit-Red; Advanced Cell Diagnostics).

Protein coding potential

Transcripts for *VINAS* (1500026H17Rik, NCBI Ref. Seq. NR_130956.1, Ensemble ID# ENSMUST00000181598) were synthesized by Genewiz. For *in vitro* validation of peptide coding potential, *VINAS* transcript was cloned upstream of p3xFLAG-CMV-14 expression vector (Sigma, E7908) using EcoRI restriction site. 293T cells were transfected with 500ng plasmid using Lipofectamine 2000 (Invitrogen) and protein lysate was isolated 72hrs post-transfection, followed by immunoblotting for FLAG Tag (Cell Signaling, 8146).

Molecular cloning for *VINAS* overexpression

For overexpression studies, the *VINAS* transcript synthesized by Genewiz, Inc was cloned in a pCDNA.3 plasmid using the EcoRI restriction site. The integration was validated by DNA sequencing. For transfection studies in ECs, 0.25 ug plasmid/well (12 wells plate) was used in combination with Lipofectamine 3000 according to the manufacturer's instructions.

Cell Culture and Transfection

Mouse endothelial cells (b.End.3, ATCC, CRL-2299) and MOVAS mouse aortic smooth muscle cells (ATCC, CRL-279) were cultured in DMEM medium with 10% FBS and 1% Penicilin-Streptomycin. HUVECs (Lonza, cc-2159) were cultured in endothelial cell growth medium EGM®-2 (Lonza, cc-3162). Cells passaged less than seven times were used for all experiments. Bone marrow was isolated from the femur and tibia of C57BL/6 mice and cultured in IMDM medium supplemented with 10 ng/ml mMCSF (mouse macrophage colony stimulation factor, (416ML, R&D), 10% FBS and 1% Penicilin-Streptomycin. Medium was changed every 2 days and cells were used in experiments after at 7-10 days in culture. Transfection was performed using Lipofectamine 3000 (Invitrogen, 11668-019) as described in manufacturer's protocol, and customized GapmeRs for *VINAS* (Qiagen, 25nmol except when mentioned differently) or negative control #1 (Qiagen). Cells were allowed to grow for 36 hours before treatment with recombinant human TNF-α (210-TA/CF, R&D Systems), IL-1B (401-ML, R&D Systems) or lipopolysaccharides (LPS, O26:B6 E. coli; SIGMAMilipore L2654) for various times, according to the experiment: Western blot, 16 hours; real-time qPCR, 6 hours.

Cell adhesion assay

ECs grown in 24-well plates were transfected with gapmeRs. After 35 hours, 20 ng/ml TNF-α was added for 5 hours. PBMCs were isolated from C57BL6 mice, washed suspended at 5×10^6 cells/ml in medium with 5 μM of Calcein AM (C3100MP; Invitrogen). Cells were kept in an incubator containing 5% CO2 at 37°C for 30 minutes. The labeling reaction was stopped by the addition of the cell growth medium, and cells were washed with growth medium twice and resuspended in growth medium at 5×10^5 cells/ml. After 4 hours of TNF-α treatment, ECs were washed once with DMEM growth medium, and 500 μl Calcein AM–loaded PBMCs were added to each well. After 1 hour of incubation, non-adherent cells were removed carefully. Adherent cells were gently washed with prewarmed DMEM medium 4 times. Adherent cells were counted using a Nikon fluorescence microscope.

RNA isolation and RT-qPCR

Tissues were homogenized using TissueLyser II (Qiagen) according to manufacturer's instructions. For RNA isolation, TRIzol reagent (Invitrogen) or RNeasy kit (Qiagen) was used based on manufacturers protocol. Isolation of intimal RNA and subsequent RT-qPCR from aorta was performed as previously documented (53) (34).

Briefly, aortas were carefully flushed with PBS, followed by intima peeling using TRIzol reagent (Invitrogen, 15596018). TRIzol was flushed for 10 sec – 10 sec pause – another 10 sec flushed and collected in an Eppendorf tube (~300-400μL total) and snap frozen in liquid nitrogen. The intima specific isolation was assessed by qPCR showing enrichment of endothelial marker CD31 and macrophage marker Mac2 in the intima fraction compared to media/adventitia fraction as previously described (15) . Subsequent RT-qPCR was performed using High-Capacity cDNA Reverse Transcription kit (Applied Biosystems, 4368813). GoTaq qPCR Master Mix (Promega, A6001) was used for RT-qPCR experiments. Expression of mRNAs and lncRNA expression levels were normalized to GAPDH, HPRT, or β-actin (Aglient, AriaMx Real Time PCR System). Changes in expression were calculated using delta delta Ct method. Primer sequences are described in (**Table S1**).

Cellular fractionation

ECs fractionation for cytoplasmic and nuclear fractions was performed using the Active Motif kit (40410) according to manufacturer's protocol. RNA was harvested as described previously and cleaned up using the RNeasy kit (Qiagen). Equivalent RNA volumes of cytoplasmic and nuclear associated RNA were converted to cDNA as described previously.

Western blot

Proteins were isolated using RIPA buffer (Boston BioProdcuts, BP-115) with protease inhibitor and phosphatase inhibitors. Protein concentrations were determined using Pierce BCA assay (Thermo Scientific). 20µg protein were loaded per lane on a 4-20% Mini-PROTEAN TGX Gel (Bio-Rad, 456-1096). Separated proteins were transferred to PVDF membranes using the Transfer Turbo Blot system (Bio-Rad) and Trans-Blot Turbo RTA Transfer Kit (Bio-Rad, 170-4272). The membrane was blocked with 5% nonfat milk in TBST for 1h at room temperature. After blocking, the membrane was incubated overnight at 4 □ with antibodies against Flag Tag (Cell Signaling, 2368, 1:1000), GAPDH (Cell Signaling, 2118, 1:4000), VCAM-1 (Cell Signaling, sc-13160, 1:1000), ICAM-1 (R&D Systems BBA3), IkBa (Cell Signaling, #4812, 1:1000), b-actin (Cell Signaling, #4970, 1:3000), and phospho-IkBa (Cell Signaling, #2859, 1:1000), IL-1β (Abcam ab9722, 1:1000), MCP-1 (Abcam ab25124, 1:1000), COX-2 (Cell Signaling 12282p), p-P38MAPK (Cell Signaling 4511L, 1:1000), P38 MAPK (Cell Signaling 9212L, 1:1000),. Quantification of protein bands were performed using a luminescent image analyzer (BioRad, Chemidoc).

Immunohistology and Characterization of Atherosclerotic Lesions

To quantify atherosclerosis in LDLR-/- mice that were placed on high cholesterol diet (HCD) (Research Diets Inc., D12108C), aortic roots and aortic arch were embedded in OCT and frozen at -80°C. Serial cryostat sections (6µm) were prepared using tissue processor Leica CM3050. Lesion characterizations, including Oil Red O (ORO) staining of the thoracic-abdominal aorta and aortic root and staining for macrophages (anti-Mac2, BD Pharmingen, 553322, 1:900) T cells (anti-CD4, BD Pharmingen, 553043, 1:90; anti-CD8, (Chemicon, CBL1318, 1:100), and vascular smooth muscle cells (SM-α-actin, Sigma, F-3777, 1:500), were performed as previously described (54) (34). The staining area was measured using Image-Pro Plus software, Media Cybernetics, and CD4+ and CD8+ cells were counted manually.

Intimal RNA isolation from aorta tissue

Isolation of intimal RNA from aorta was performed as previously described in (34) (53). Briefly, aortas were carefully flushed with PBS, followed by intima peeling using TRIzol reagent (Invitrogen, 15596018). TRIzol was flushed for 10 sec – 10 sec pause – another 10 sec flushed and collected in an Eppendorf tube (~300-400µL total) and snap frozen in liquid nitrogen. The intima specific isolation was assessed in a previous study (15) by qPCR showing enrichment of endothelial marker CD31 in the intima fraction compared to media/adventitia fraction.

Lipid Profile Analysis

Lipid profile was measured as previously described (34). Briefly triglyceride levels were determined using InfinityTM Triglycerides Liquid Stable Reagent (Thermo Scientific). Total cholesterol was measured using the InfinityTM Cholesterol Reagent (Thermo Scientific) and HDL cholesterol was measured by colorimetric assay (BioAssay Systems, EnzyChromTM HDL). LDL cholesterol levels were calculated using the following formula: LDL=Total Cholesterol – HDL Cholesterol – Triglycerides divided by five. Standards were purchased from Pointe Scientific, Inc.

Animal Studies

All protocols concerning animal use were approved by the Institutional Animal Care and Use Committee at Brigham and Women's Hospital and Harvard Medical School, Boston, MA and conducted in accordance with the National Institutes of Health Guide for the Care and Use of Laboratory Animals. Studies were performed in $LDLR^{-/-}$ male mice (Jackson Laboratory, Stock#: 002207) or in C57Bl/6 mice (Charles River, Strain code#027).

Pig Atherosclerotic Samples

The study protocol included 15 male hypercholesterolemic Yorkshire swine that were placed on an HCD for up to 60 weeks. Detailed sectioning of 3-mm coronary artery segments was performed so that the gene sequencing samples were derived from the exact same portions of the coronary artery plaques used for the histology and immunohistochemistry analyses. Histology and IHC analyses included H & E, van Gieson elastin staining, smooth muscle cell α-actin, oil red-O staining (ORO), picrosirius red staining, CD31 and CD45 cells as described in (55) (15).

Human Atherosclerotic Specimens

RNA was isolated from human carotid atherosclerotic lesions that were obtained from the Division of Cardiovascular Medicine, Brigham and Women's Hospital in accordance with the Institutional Review Board-approved protocol for use of discarded human tissues (protocol #2010-P-001930/2).

Statistics

Data throughout the paper are expressed as mean ± SD. Statistical differences were calculated using unpaired two-tailed Student's t-test or one-way ANOVA with Bonferroni correction for multiple comparisons. A probability of $p<0.05$ was considered statistically significant. Ns, not significant; * $p<0.05$; ** $p<0.01$; *** $p<0.001$; **** $p<0.0001$. For illustration of differentially expressed genes Prism GraphPad software (V.7.0a) was used.

Author Contributions:

Conceived the hypothesis (M.W.F. and V.S.), performed the experiments (V.S., H.Z., J.B.P., D.Y., and Y.T.), designed and interpreted the results (V.S., H.Z., J.B.P., S.H., G.S. P.S., P.L., and M.W.F.), wrote the manuscript (V.S. and M.W.F.).

Acknowledgments:

We would like to thank J. Hutchinson and L. Pantano (Harvard Chan Bioinformatics Core, Harvard T.H. Chan School of Public Health, Boston, MA) for assistance with RNA-seq analysis. This work was supported by the NIH (HL115141, HL134849, HL148207, HL148355, HL153356 to M.W.F.; the Arthur K. Watson Charitable Trust (to M.W.F.), the Dr. Ralph and Marian Falk Medical Research Trust (to M.W.F.), the American Heart Association (18SFRN33900144 and 20SFRN35200163 to M.W.F.), the Sarnoff Foundation Fellowship Award (J.B.P). PL received funding from the National Heart, Lung, and Blood Institute [R01HL080472], American Heart Association [18CSA34080399], and RRM Charitable Fund.

544

545

546

References

1. Libby P. Inflammation in atherosclerosis. *Arterioscler Thromb Vasc Biol.* 2012;32(9):2045-51.
2. Wolf D, and Ley K. Immunity and Inflammation in Atherosclerosis. *Circ Res.* 2019;124(2):315-27.
3. Virchow R. Cellular pathology. As based upon physiological and pathological histology. Lecture XVI--Atheromatous affection of arteries. 1858. *Nutr Rev.* 1989;47(1):23-5.
4. Ridker PM, Everett BM, Thuren T, MacFadyen JG, Chang WH, Ballantyne C, et al. Antiinflammatory Therapy with Canakinumab for Atherosclerotic Disease. *N Engl J Med.* 2017;377(12):1119-31.
5. Nahrendorf M. Myeloid cell contributions to cardiovascular health and disease. *Nat Med.* 2018;24(6):711-20.
6. Libby P. Mechanisms of acute coronary syndromes and their implications for therapy. *N Engl J Med.* 2013;368(21):2004-13.
7. Mullick AE, Soldau K, Kiosses WB, Bell TA, 3rd, Tobias PS, and Curtiss LK. Increased endothelial expression of Toll-like receptor 2 at sites of disturbed blood flow exacerbates early atherogenic events. *J Exp Med.* 2008;205(2):373-83.
8. Gimbrone MA, Jr., and Garcia-Cardena G. Endothelial Cell Dysfunction and the Pathobiology of Atherosclerosis. *Circ Res.* 2016;118(4):620-36.
9. Doran AC, Meller N, and McNamara CA. Role of smooth muscle cells in the initiation and early progression of atherosclerosis. *Arterioscler Thromb Vasc Biol.* 2008;28(5):812-9.
10. Ley K, Miller YI, and Hedrick CC. Monocyte and macrophage dynamics during atherogenesis. *Arterioscler Thromb Vasc Biol.* 2011;31(7):1506-16.
11. Simion V, Haemmig S, and Feinberg MW. LncRNAs in vascular biology and disease. *Vascul Pharmacol.* 2018.
12. Aryal B, and Suarez Y. Non-coding RNA regulation of endothelial and macrophage functions during atherosclerosis. *Vascul Pharmacol.* 2018.
13. Haemmig S, Simion V, and Feinberg MW. Long Non-Coding RNAs in Vascular Inflammation. *Front Cardiovasc Med.* 2018;5:22.
14. Haemmig S, Simion V, Yang D, Deng Y, and Feinberg MW. Long noncoding RNAs in cardiovascular disease, diagnosis, and therapy. *Curr Opin Cardiol.* 2017;32(6):776-83.
15. Haemmig S, Yang D, Sun X, Das D, Ghaffari S, Molinaro R, et al. Long noncoding RNA SNHG12 integrates a DNA-PK-mediated DNA damage response and vascular senescence. *Sci Transl Med.* 2020;12(531).
16. Leisegang MS, Fork C, Josipovic I, Richter FM, Preussner J, Hu J, et al. Long Noncoding RNA MANTIS Facilitates Endothelial Angiogenic Function. *Circulation.* 2017;136(1):65-79.
17. Mahmoud AD, Ballantyne MD, Miscianinov V, Pinel K, Hung J, Scanlon JP, et al. The Human-Specific and Smooth Muscle Cell-Enriched LncRNA SMILR Promotes Proliferation by Regulating Mitotic CENPF mRNA and Drives Cell-Cycle Progression Which Can Be Targeted to Limit Vascular Remodeling. *Circ Res.* 2019;125(5):535-51.
18. Stapleton K, Das S, Reddy MA, Leung A, Amaram V, Lanting L, et al. Novel Long Noncoding RNA, Macrophage Inflammation-Suppressing Transcript (MIST), Regulates

Macrophage Activation During Obesity. *Arterioscler Thromb Vasc Biol.* 2020;40(4):914-28.
19. Sallam T, Jones MC, Gilliland T, Zhang L, Wu X, Eskin A, et al. Feedback modulation of cholesterol metabolism by the lipid-responsive non-coding RNA LeXis. *Nature.* 2016;534(7605):124-8.
20. Sallam T, Jones M, Thomas BJ, Wu X, Gilliland T, Qian K, et al. Transcriptional regulation of macrophage cholesterol efflux and atherogenesis by a long noncoding RNA. *Nat Med.* 2018;24(3):304-12.
21. Tontonoz P, Wu X, Jones M, Zhang Z, Salisbury D, and Sallam T. Long noncoding RNA facilitated gene therapy reduces atherosclerosis in a murine model of familial hypercholesterolemia. *Circulation.* 2017;136(8):776-8.
22. Hu Y-W, Guo F-X, Xu Y-J, Li P, Lu Z-F, McVey DG, et al. Long noncoding RNA NEXN-AS1 mitigates atherosclerosis by regulating the actin-binding protein NEXN. *The Journal of clinical investigation.* 2019;129(3).
23. Li H, Cybulsky MI, Gimbrone MA, Jr., and Libby P. An atherogenic diet rapidly induces VCAM-1, a cytokine-regulatable mononuclear leukocyte adhesion molecule, in rabbit aortic endothelium. *Arterioscler Thromb.* 1993;13(2):197-204.
24. Libby P. Mechanisms of acute coronary syndromes. *N Engl J Med.* 2013;369(9):883-4.
25. de Gaetano M, Crean D, Barry M, and Belton O. M1- and M2-Type Macrophage Responses Are Predictive of Adverse Outcomes in Human Atherosclerosis. *Front Immunol.* 2016;7:275.
26. Williams HJ, Fisher EA, and Greaves DR. Macrophage differentiation and function in atherosclerosis: opportunities for therapeutic intervention? *J Innate Immun.* 2012;4(5-6):498-508.
27. Cho KY, Miyoshi H, Kuroda S, Yasuda H, Kamiyama K, Nakagawara J, et al. The phenotype of infiltrating macrophages influences arteriosclerotic plaque vulnerability in the carotid artery. *J Stroke Cerebrovasc Dis.* 2013;22(7):910-8.
28. Shaikh S, Brittenden J, Lahiri R, Brown PA, Thies F, and Wilson HM. Macrophage subtypes in symptomatic carotid artery and femoral artery plaques. *Eur J Vasc Endovasc Surg.* 2012;44(5):491-7.
29. Han J, Liu S, Sun Z, Zhang Y, Zhang F, Zhang C, et al. LncRNAs2Pathways: Identifying the pathways influenced by a set of lncRNAs of interest based on a global network propagation method. *Sci Rep.* 2017;7:46566.
30. Hajra L, Evans AI, Chen M, Hyduk SJ, Collins T, and Cybulsky MI. The NF-κB signal transduction pathway in aortic endothelial cells is primed for activation in regions predisposed to atherosclerotic lesion formation. *Proceedings of the National Academy of Sciences.* 2000;97(16):9052-7.
31. Baker RG, Hayden MS, and Ghosh S. NF-κB, inflammation, and metabolic disease. *Cell metabolism.* 2011;13(1):11-22.
32. Bäck M, and Hansson GK. Anti-inflammatory therapies for atherosclerosis. *Nature Reviews Cardiology.* 2015;12(4):199.
33. Gareus R, Kotsaki E, Xanthoulea S, van der Made I, Gijbels MJ, Kardakaris R, et al. Endothelial cell-specific NF-κB inhibition protects mice from atherosclerosis. *Cell metabolism.* 2008;8(5):372-83.

34. Sun X, He S, Wara AKM, Icli B, Shvartz E, Tesmenitsky Y, et al. Systemic delivery of microRNA-181b inhibits nuclear factor-kappaB activation, vascular inflammation, and atherosclerosis in apolipoprotein E-deficient mice. *Circ Res.* 2014;114(1):32-40.
35. Morris JB, Olzinski AR, Bernard RE, Aravindhan K, Mirabile RC, Boyce R, et al. p38 MAPK inhibition reduces aortic ultrasmall superparamagnetic iron oxide uptake in a mouse model of atherosclerosis: MRI assessment. *Arteriosclerosis, thrombosis, and vascular biology.* 2008;28(2):265-71.
36. Seeger FH, Sedding D, Langheinrich AC, Haendeler J, Zeiher AM, and Dimmeler S. Inhibition of the p38 MAP kinase in vivo improves number and functional activity of vasculogenic cells and reduces atherosclerotic disease progression. *Basic research in cardiology.* 2010;105(3):389-97.
37. Sarov-Blat L, Morgan JM, Fernandez P, James R, Fang Z, Hurle MR, et al. Inhibition of p38 mitogen-activated protein kinase reduces inflammation after coronary vascular injury in humans. *Arteriosclerosis, thrombosis, and vascular biology.* 2010;30(11):2256-63.
38. Elkhawad M, Rudd JH, Sarov-Blat L, Cai G, Wells R, Davies LC, et al. Effects of p38 mitogen-activated protein kinase inhibition on vascular and systemic inflammation in patients with atherosclerosis. *JACC: Cardiovascular Imaging.* 2012;5(9):911-22.
39. Cargnello M, and Roux PP. Activation and function of the MAPKs and their substrates, the MAPK-activated protein kinases. *Microbiol Mol Biol Rev.* 2011;75(1):50-83.
40. Hommes DW, Peppelenbosch MP, and van Deventer SJ. Mitogen activated protein (MAP) kinase signal transduction pathways and novel anti-inflammatory targets. *Gut.* 2003;52(1):144-51.
41. Roux PP, and Blenis J. ERK and p38 MAPK-activated protein kinases: a family of protein kinases with diverse biological functions. *Microbiol Mol Biol Rev.* 2004;68(2):320-44.
42. Liu T, Zhang L, Joo D, and Sun SC. NF-kappaB signaling in inflammation. *Signal Transduct Target Ther.* 2017;2.
43. Xie Y, Xie K, Gou Q, and Chen N. IkappaB kinase alpha functions as a tumor suppressor in epithelial-derived tumors through an NF-kappaB-independent pathway (Review). *Oncol Rep.* 2015;34(5):2225-32.
44. Shan Y, Ma J, Pan Y, Hu J, Liu B, and Jia L. LncRNA SNHG7 sponges miR-216b to promote proliferation and liver metastasis of colorectal cancer through upregulating GALNT1. *Cell Death Dis.* 2018;9(7):722.
45. Wu DM, Wang S, Wen X, Han XR, Wang YJ, Shen M, et al. LncRNA SNHG15 acts as a ceRNA to regulate YAP1-Hippo signaling pathway by sponging miR-200a-3p in papillary thyroid carcinoma. *Cell Death Dis.* 2018;9(10):947.
46. Denzler R, Agarwal V, Stefano J, Bartel DP, and Stoffel M. Assessing the ceRNA hypothesis with quantitative measurements of miRNA and target abundance. *Mol Cell.* 2014;54(5):766-76.
47. Iyer SS, Ghaffari AA, and Cheng G. Lipopolysaccharide-mediated IL-10 transcriptional regulation requires sequential induction of type I IFNs and IL-27 in macrophages. *J Immunol.* 2010;185(11):6599-607.
48. Mukherjee S, Chen LY, Papadimos TJ, Huang S, Zuraw BL, and Pan ZK. Lipopolysaccharide-driven Th2 cytokine production in macrophages is regulated by both MyD88 and TRAM. *J Biol Chem.* 2009;284(43):29391-8.

49. Du M, Yuan L, Tan X, Huang D, Wang X, Zheng Z, et al. The LPS-inducible lncRNA Mirt2 is a negative regulator of inflammation. *Nat Commun.* 2017;8(1):2049.
50. Tone M, Powell MJ, Tone Y, Thompson SA, and Waldmann H. IL-10 gene expression is controlled by the transcription factors Sp1 and Sp3. *J Immunol.* 2000;165(1):286-91.
51. Dobin A, Davis CA, Schlesinger F, Drenkow J, Zaleski C, Jha S, et al. STAR: ultrafast universal RNA-seq aligner. *Bioinformatics.* 2013;29(1):15-21.
52. Liao Y, Smyth GK, and Shi W. featureCounts: an efficient general purpose program for assigning sequence reads to genomic features. *Bioinformatics.* 2014;30(7):923-30.
53. Sun X, Icli B, Wara AK, Belkin N, He S, Kobzik L, et al. MicroRNA-181b regulates NF-kappaB-mediated vascular inflammation. *J Clin Invest.* 2012;122(6):1973-90.
54. Cao Z, Wara AK, Icli B, Sun X, Packard RR, Esen F, et al. Kruppel-like factor KLF10 targets transforming growth factor-beta1 to regulate CD4(+)CD25(-) T cells and T regulatory cells. *J Biol Chem.* 2009;284(37):24914-24.
55. Koskinas KC, Chatzizisis YS, Papafaklis MI, Coskun AU, Baker AB, Jarolim P, et al. Synergistic effect of local endothelial shear stress and systemic hypercholesterolemia on coronary atherosclerotic plaque progression and composition in pigs. *Int J Cardiol.* 2013;169(6):394-401.

819 **Tabel S1. Primers sequences**

Primers	forward	reverse
VINAS	TAGGAAGCCCGAGTTTCTGGA	GTTTCCAGATGTCCTTCACAGC
DEPDC4	CCAGGAACCGTAGAGATGGC	CCACTTGGGCCTGAAGAGAG
GAPDH	AGGTCGGTGTGAACGGATTTG	TGTAGACCATGTAGTTGAGGTCA
COX-2	TGTGACTGTACCCGGACTGG	TGCACATTGTAAGTAGGTGGAC
MCP-1	GCTGGAGCATCCACGTGTT	ATCTTGCTGGTGAATGAGTAGCA
TNF-α	CTGGATGTCAATCAACAATGGGA	ACTAGGGTGTGAGTGTTTTCTGT
VCAM-1	CAACATGTGGCTCTGGGAAG	GCCAAACACTTGACCGTGAC
ICAM-1	TTCTCATGCCGCACAGAACT	TGTCGAGCTTTGGGATGGTA
E-selectin	ATGCCTCGCGCTTTCTCTC	GTAGTCCCGCTGACAGTATGC
MCP-1	TTAAAAACCTGGATCGGAACCAA	GCATTAGCTTCAGATTTACGGGT
COX-2	CATCCCCTTCCTGCGAAGTT	CATGGGAGTTGGGCAGTCAT
U6	CTCGCTTCGGCAGCACA	AACGCTTCACGAATTTGCGT
IL-1β	ATGCCACCTTTTGACAGTGATG	AGCTTCTCCACAGCCACAAT
COX2	TTCAACACACTCTATCACTGGC	AGAAGCGTTTGCGGTACTCAT

820

821

822

823 **Table S2. Transcription factors binding to *VINAS* and DEPDC4 promoters**

VINAS	**DEPDC4**
Elk-1	AP-2
Sp1	AP-2-alpha
Pegasus	AP-2-gamma
Sp1	AP-2
SIF	AP-2-alpha
E4F1	AP-2-gamma
AP-2-alpha	Ets

AP-2	SIF
AP-2-gamma	E4F1
AP-2-alpha	AP-2
AP-2	Pax4-PD
SIF	Sp1
PEA2	TEF
AP-2	AP-2-alpha
Pegasus	AP-2-gamma
AP-2-alpha	Ap-2
AP-2-gamma	STAT1-hs
AP-2	Pax4-PD
RAR	ZNF217
ARP-1	COUP-TF
H3abp	AP-2
AP-1	TFII-I
AP-2-alpha	AP-2-alpha
H4TF2	Pegasus
AP-2	AP-2-alpha
Pegasus	AP-2-gamma
AP-2-alpha	AP-2
AP-2-gamma	AP-2-alpha
AP-2-alpha	AP-2-gamma
AP-2-gamma	Nkx-3.2
AP-2	Elk-1
AP-2	COUP-TF
AP-2-alpha	Sp1

AP-2-gamma	Elk-1
AP-2	AP-2
AP-2-alpha	Sp1
Sp1	Sp1
Pegasus	Hox15
ENKTF1	AP-2-alpha
E4F1	AP-2
Pegasus	AP-2-alpha
STAT1-hs	Ets
STAT1-hs	Ets
Pegasus	Elk-1
STAT1-hs	ENKTF1
Ets	EGR-1
Ets	AP-2
H3abp	AP-2-alpha
ATF-CREB	AP-2-gamma
TEF	Pegasus
LRF-1	Pegasus
E4F1	Sp1
E4F1	Pax4-PD
LRF-1	ZNF219
Erg	H4TF2
STAT1-hs	AP-2

ATF-CREB	Pegasus
H3abp	STAT5A-hs
EF-1	STAT6-hs
EF-1A	MBF-1
E1A-F	Ets
Net_SAP2	AP-2-alpha
Elk-1	AP-2-gamma
STAT1-hs	AP-2
HNF-4	AP-2-alpha
Pegasus	AP-2-gamma
AP-2	H3abp
AP-2-alpha	ATF-CREB
AP-2-gamma	TEF
Pegasus	LRF-1
Sp1	E4F1
GCF	E4F1
AP-2	LRF-1
AP-2-alpha	Erg
AP-2-gamma	STAT1-hs
	ATF-CREB
	H3abp
	Ets
	EF-1A
	E1A-F
	PEA3
	Net_SAP2

	Elk-1
	Sp1
	STAT1-hs
	CP2
	AP-2-alpha
	AP-2-gamma
	AP-2
	E2A
	Sp1
	Pax4-PD
	ZNF219

824

Fig. 1

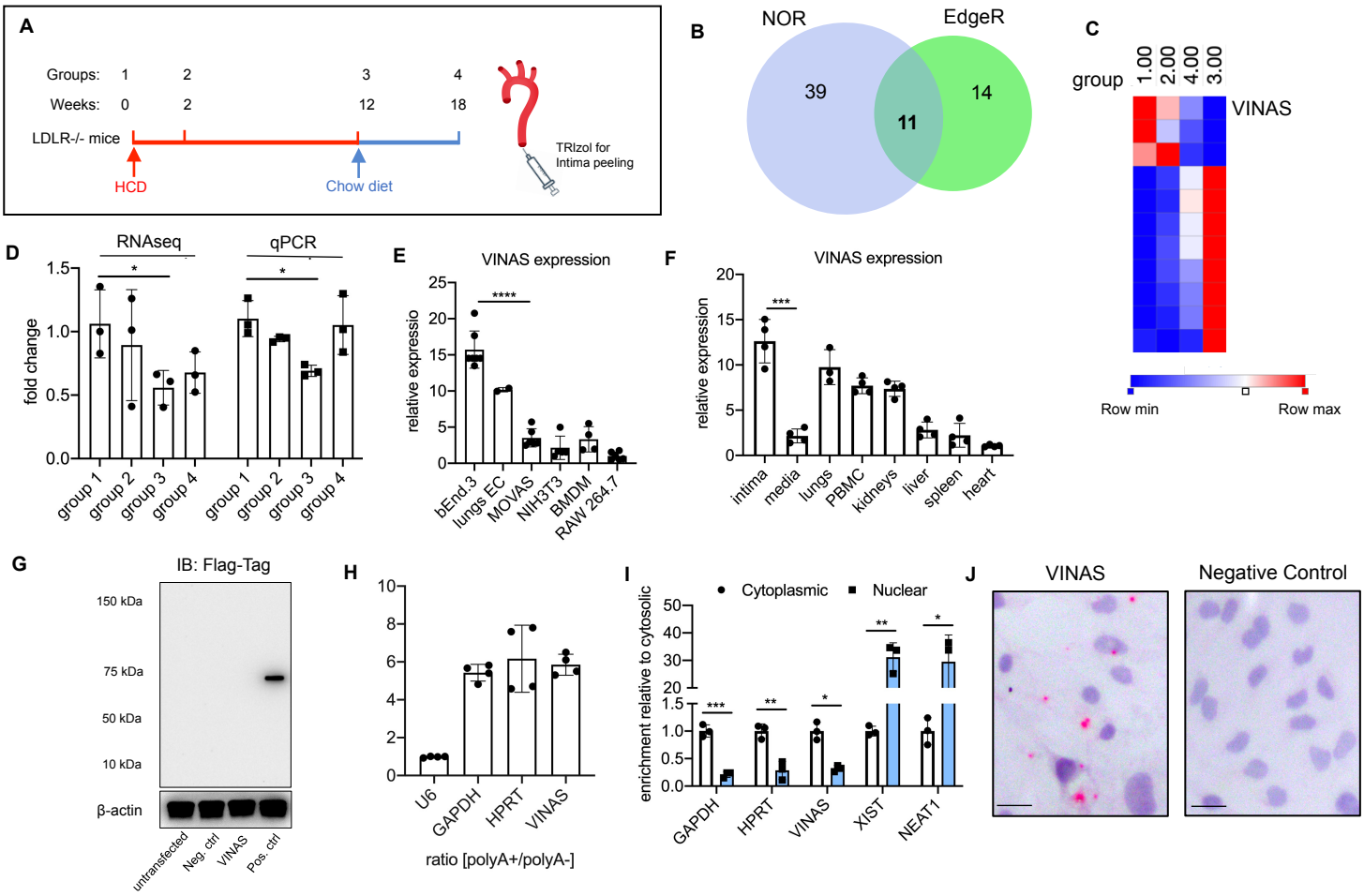
A
Groups: 1 2 3 4
Weeks: 0 2 12 18
LDLR-/- mice
HCD
Chow diet
TRIzol for
Intima peeling
B
NOR
EdgeR
39
11
14
C
group 1.00 2.00 4.00 3.00
VINAS
Row min
Row max
D
RNAseq
qPCR
fold change
group 1
group 2
group 3
group 4
E
VINAS expression
relative expressio
bEnd.3
lungs EC
MOVAS
NIH3T3
BMDM
RAW 264.7
F
VINAS expression
relative expression
intima
media
lungs
PBMC
kidneys
liver
spleen
heart
G
IB: Flag-Tag
150 kDa
75 kDa
50 kDa
10 kDa
β-actin
untransfected
Neg. ctrl
VINAS
Pos. ctrl
H
U6
GAPDH
HPRT
VINAS
ratio [polyA+/polyA-]
I
Cytoplasmic
Nuclear
enrichment relative to cytosolic
GAPDH
HPRT
VINAS
XIST
NEAT1
J
VINAS
Negative Control

Fig. 1. Identification of the lncRNA *VINAS* in lesional intima. **A.** RNA derived from aortic intima of $LDLR^{-/-}$ mice (n=3; each sample represents RNA pooled from two mice) that were placed on an HCD for 0 weeks (group 1), 2 weeks (group 2), 12 weeks (group 3), and 18 weeks after 6 weeks of resumption of a normal chow diet (group 4). **B.** Venn diagram displays significantly dysregulated lncRNAs in genome-wide RNA-Seq profiling using EdgeR and NOR showing intersecting hits (n=11), uniquely identified in EdgeR (n=14) or NOR (n=39), (log2-fold change (1.5); FDR<0.05). **C.** Heatmap for 11 lncRNAs that were dynamically regulated with progression and regression of atherosclerosis (n=3). **D.** RNA-Seq results for *VINAS* across groups 1-4 obtained by RNAseq analysis and verified by RT-qPCR (n=3). **E.** RT-qPCR expression analysis for *VINAS* in different cell types (n=3). **F.** *VINAS* expression in body organs and PBMCs of 24 weeks old C57BL/6 mice (n=4) **G.** To test the coding potential, *VINAS* sequence was cloned upstream of 3xFlag-Tag cassette, transfected in 293T cells, and immunoblotted for Flag antibody. Positive control was provided with the kit (representative of 3 experiments). **H.** RNA from mouse ECs was isolated for polyA+ and polyA- enriched RNA and analyzed by RT-qPCR. (n=3). **I.** RT-qPCR analysis for RNA derived from mouse ECs separated into cytoplasmic and nuclear fractions and normalized to the cytoplasmic fraction (n=3). **J.** RNA-*in situ* hybridization for negative control- and *VINAS*-probes on PFA-fixed mouse ECs; Scale bar, 5 μm. For all panels, values are mean ± SD; Statistical differences were calculated using unpaired two-tailed Student's t-test for all panels except for multiple comparisons (E, F) where one-way ANOVA with Bonferroni correction was used. *p < 0.05, **p<0.01; ***p<0.001.

Fig. 2

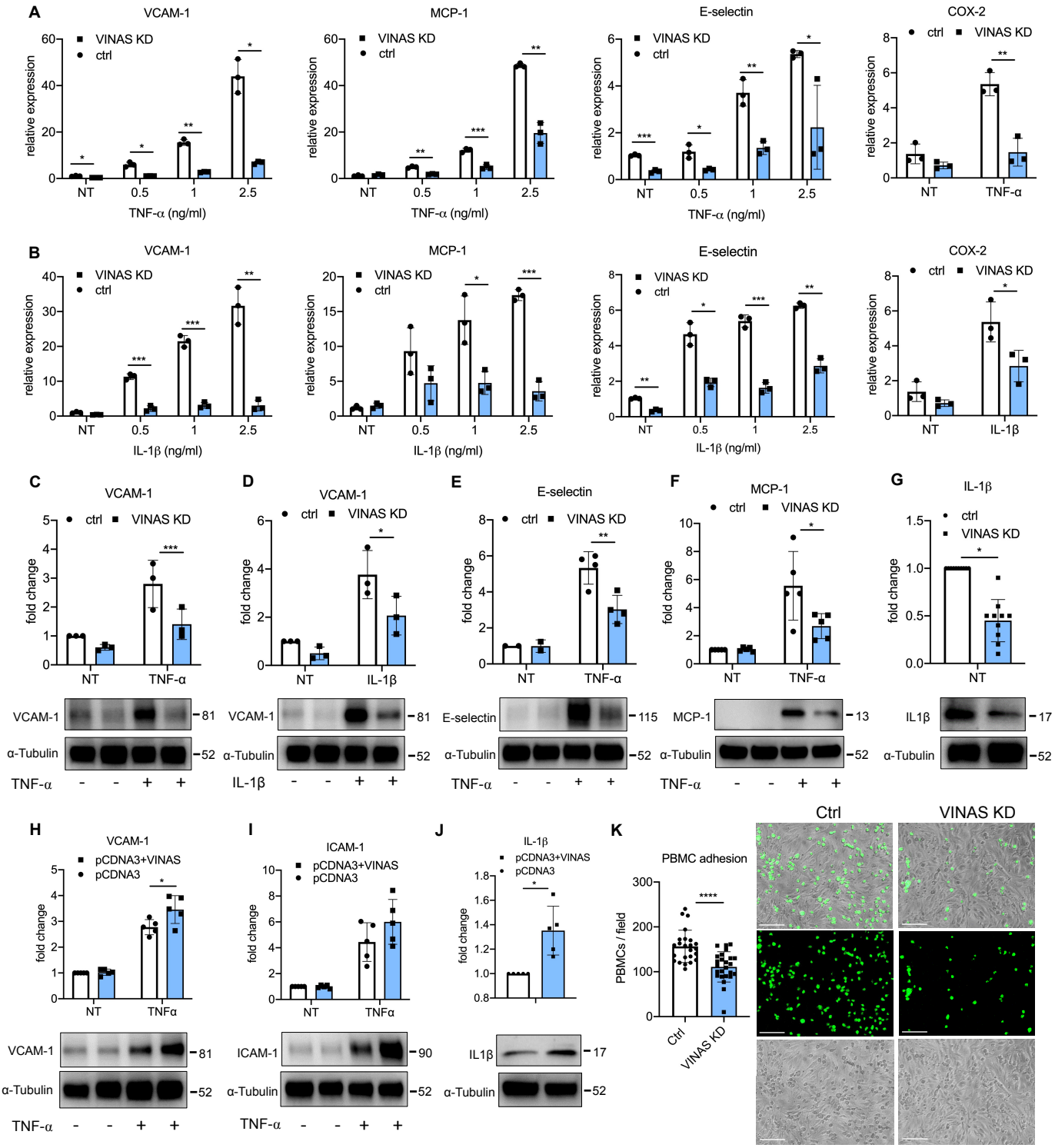
A
VCAM-1
MCP-1
E-selectin
COX-2
VINAS KD
ctrl
relative expression
TNF-α (ng/ml)
NT
0.5
1
2.5
TNF-α
B
IL-1β (ng/ml)
IL-1β
C
D
E
F
G
fold change
VCAM-1
E-selectin
MCP-1
IL1β
α-Tubulin
TNF-α
IL-1β
H
I
J
K
pCDNA3+VINAS
pCDNA3
ICAM-1
TNFα
PBMC adhesion
PBMCs / field
Ctrl
VINAS KD

Fig. 2. *VINAS* regulates inflammatory markers in endothelial cells. *VINAS* knockdown decreases the mRNA levels of VCAM-1, E-selectin, MCP-1, and COX2 in mouse ECs activated with TNF-α **(A)** and IL-1β **(B);** n=3. *VINAS* silencing decreases the protein expression of VCAM-1 (**C, D**, n=3), E-selectin (**E**; n=4), MCP-1 (**F**, n=5), and IL-1β (**G**; n=10) in basal conditions or after activation with 20 ng/ml of TNF-α or IL-1β. *VINAS* overexpression increases the protein expression of VCAM-1 (**H**) ICAM-1 (**I**) and IL-1β **(J)** in mouse ECs non-treated or activated with 20 ng/ml of TNF-α (n=5). **K.** *VINAS* knockdown decrease the PBMCs adhesion to mouse ECs activated with TNF-α for 4 hours (5 ng/ml, representative of three experiments; Scale bar, 50 μm. For all panels, values are mean ± SD; Statistical differences were calculated using unpaired two-tailed Student's t-test for all panels. *p<0.05, **p<0.01; ***p<0.001; ****p<0.0001.

Fig. 3

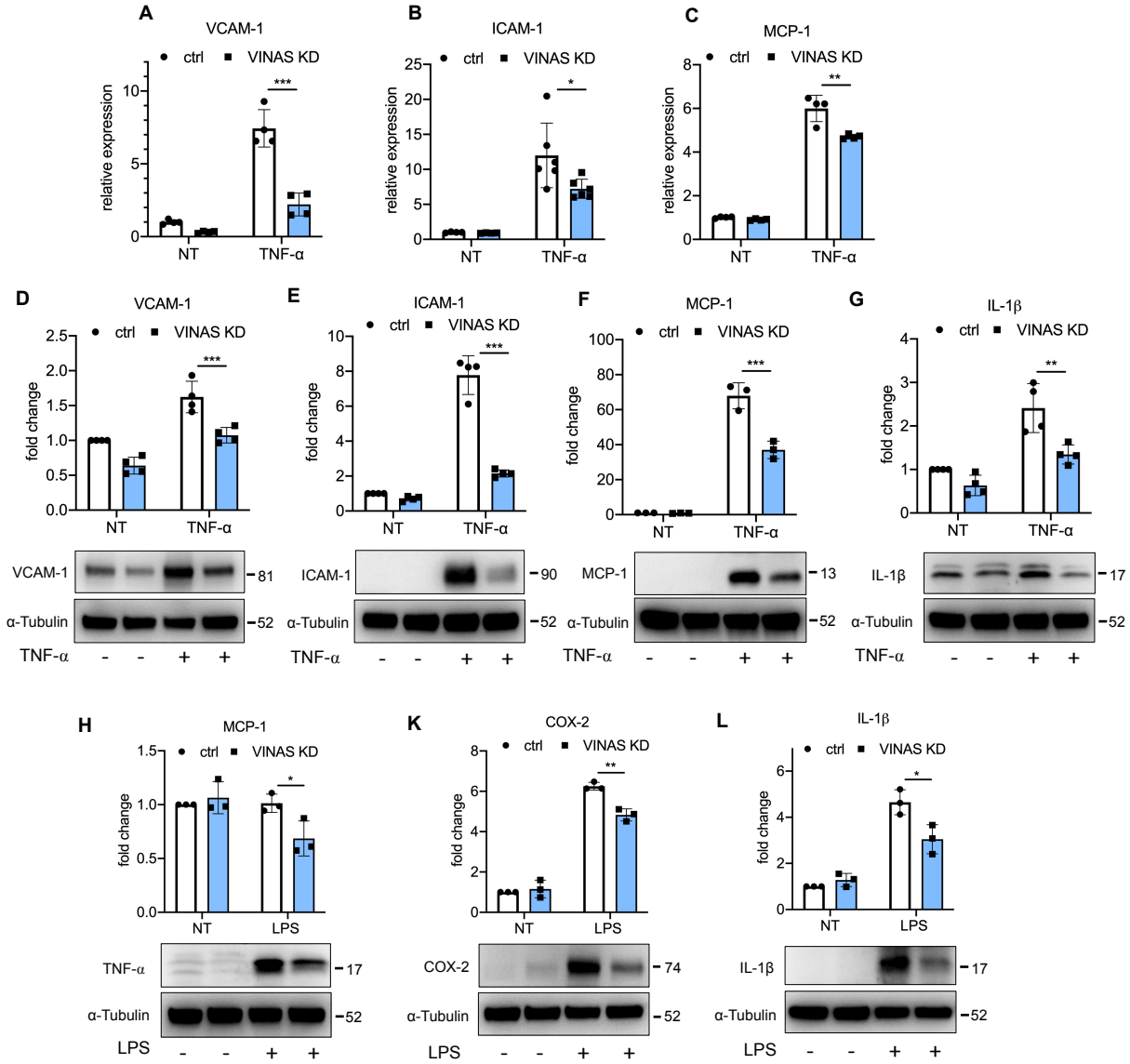
A
VCAM-1
ctrl
VINAS KD
relative expression
NT
TNF-α
B
ICAM-1
C
MCP-1
D
VCAM-1
fold change
E
ICAM-1
F
MCP-1
G
IL-1β
VCAM-1
ICAM-1
MCP-1
IL-1β
α-Tubulin
TNF-α
H
MCP-1
K
COX-2
L
IL-1β
LPS

Fig. 3. *VINAS* knockdown decrease inflammation in SMC and BMDM. *VINAS* knockdown decrease mRNA levels of VCAM-1 (**A**; n=4), ICAM-1 (**B**; n=6), and MCP-1 (**C**; n=4) in MOVAS smooth muscle cells (SMC) stimulated with 5 ng/ml TNF-α. *VINAS* knockdown decrease the protein expression of VCAM-1 (**D**; n=4), ICAM-1 (**E**; n=4),, MCP-1 (**F**; n=3), IL-1β (**G**; n=4), in in MOVAS smooth muscle cells stimulated with 20 ng/ml TNF-α. *VINAS* knockdown decreases the protein expression of MCP-1 (**H**), COX-2 (**K**), and IL-1β (**L**) in bone marrow-derived macrophages (BMDM) stimulated with 50 ng/ml LPS (n=3). For all panels, values are mean ± SD; Statistical differences were calculated using unpaired two-tailed Student's t-test for all panels. *$p < 0.05$, **$p<0.01$; ***$p<0.001$.

Fig. 4

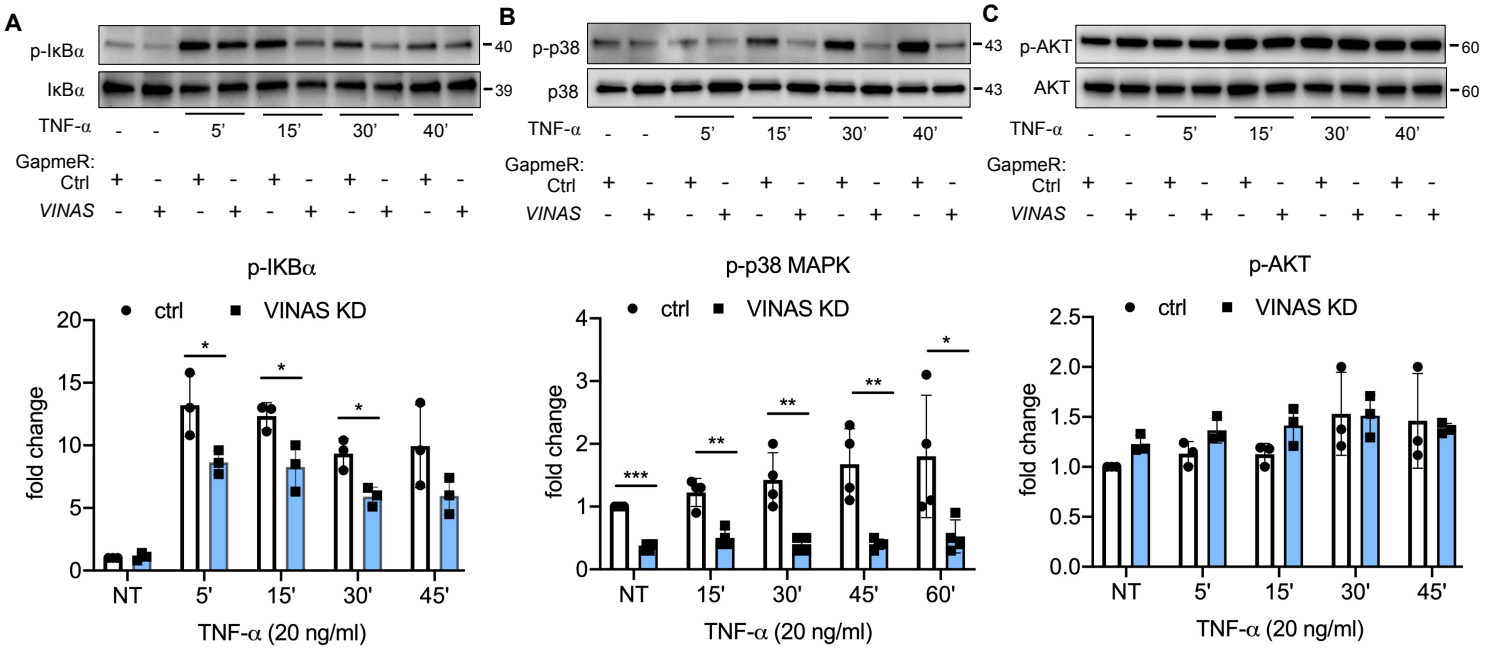
A
p-IκBα
IκBα
40
39
TNF-α - - 5' 15' 30' 40'
GapmeR:
Ctrl + - + - + - + - + -
VINAS - + - + - + - + - +
B
p-p38
p38
43
43
TNF-α - - 5' 15' 30' 40'
GapmeR:
Ctrl + - + - + - + - + -
VINAS - + - + - + - + - +
C
p-AKT
AKT
60
60
TNF-α - - 5' 15' 30' 40'
GapmeR:
Ctrl + - + - + - + - + -
VINAS - + - + - + - + - +

p-IKBα
ctrl
VINAS KD
fold change
20
15
10
5
0
*
*
*
NT
5'
15'
30'
45'
TNF-α (20 ng/ml)

p-p38 MAPK
ctrl
VINAS KD
fold change
4
3
2
1
0
***
**
**
**
*
NT
15'
30'
45'
60'
TNF-α (20 ng/ml)

p-AKT
ctrl
VINAS KD
fold change
2.5
2.0
1.5
1.0
0.5
0.0
NT
5'
15'
30'
45'
TNF-α (20 ng/ml)

Fig. 4. *VINAS* knockdown regulates NF-κB and p38 MAPK signaling pathways. Mouse ECs were transfected with VINAS gapmeRs and activated with TNF--α (20 ng/ml) for 5, 15, 30, 45 and 60 minutes. Phosphorylation of IKB-α (**A**; n=3), p-38 MAPK (**B**; n=4), and AKT (**C**; n=3) were assessed by Western Blot. For all panels, values are mean ± SD; Statistical differences for all panels were calculated using one-way ANOVA with Bonferroni correction. *$p < 0.05$, **$p<0.01$; ***$p<0.001$.

Fig. 5

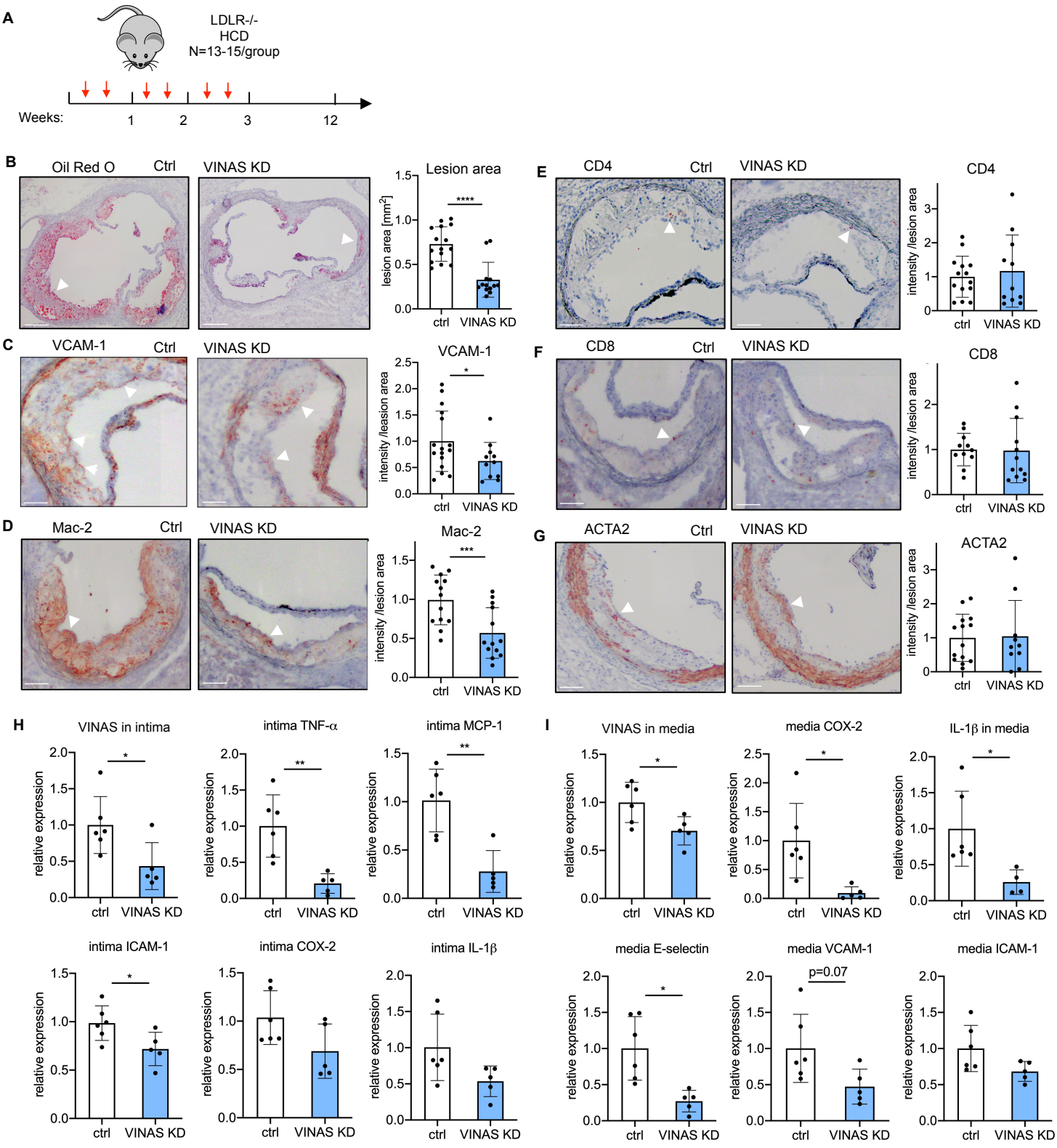
A
LDLR-/-
HCD
N=13-15/group
Weeks:
1
2
3
12
B
Oil Red O
Ctrl
VINAS KD
Lesion area
lesion area [mm²]
****
ctrl
VINAS KD
C
VCAM-1
Ctrl
VINAS KD
VCAM-1
intensity /lesion area
*
ctrl
VINAS KD
D
Mac-2
Ctrl
VINAS KD
Mac-2
intensity /lesion area
***
ctrl
VINAS KD
E
CD4
Ctrl
VINAS KD
CD4
intensity /lesion area
ctrl
VINAS KD
F
CD8
Ctrl
VINAS KD
CD8
intensity /lesion area
ctrl
VINAS KD
G
ACTA2
Ctrl
VINAS KD
ACTA2
intensity /lesion area
ctrl
VINAS KD
H
VINAS in intima
intima TNF-α
intima MCP-1
intima ICAM-1
intima COX-2
intima IL-1β
relative expression
ctrl
VINAS KD
I
VINAS in media
media COX-2
IL-1β in media
media E-selectin
media VCAM-1
p=0.07
media ICAM-1
relative expression
ctrl
VINAS KD

Fig. 5. *In vivo* knockdown of *VINAS* inhibits atherosclerotic lesion formation by decreasing vascular inflammation. **A.** LDLR$^{-/-}$ mice were i.v. injected with vehicle control-gapmeR (n=15) or *VINAS*-gapmeR (n=13) twice per week (10 mg/kg/mouse/injection) and placed on HCD for 12 weeks. Representative images and quantification for Oil Red O (Scale bar, 400 μm) (**B**), VCAM-1 (**C**), Mac-2 (**D**), CD4 (**E**), CD8 (**F**) and ACTA2 (**G**) staining (arrowhead) of the aortic sinus of LDLR$^{-/-}$ HCD mice treated with control (n=15) or *MAARS* (n=13) gapmeRs for 12 weeks; Scale bar, 100 μm. *VINAS* silencing efficiency and expression of inflammatory markers was assessed by RT-qPCR in the intima (**H**) and media (**I**) fractions of the aortic arch from control gapmeR (n=6) and *VINAS* gapmeR groups (n=5). For all panels, values are mean ± SD; Statistical differences were calculated using unpaired two-tailed Student's t-test for all panels. *p<0.05, **p<0.01; ***p<0.001; ****p<0.0001.

Fig. 6

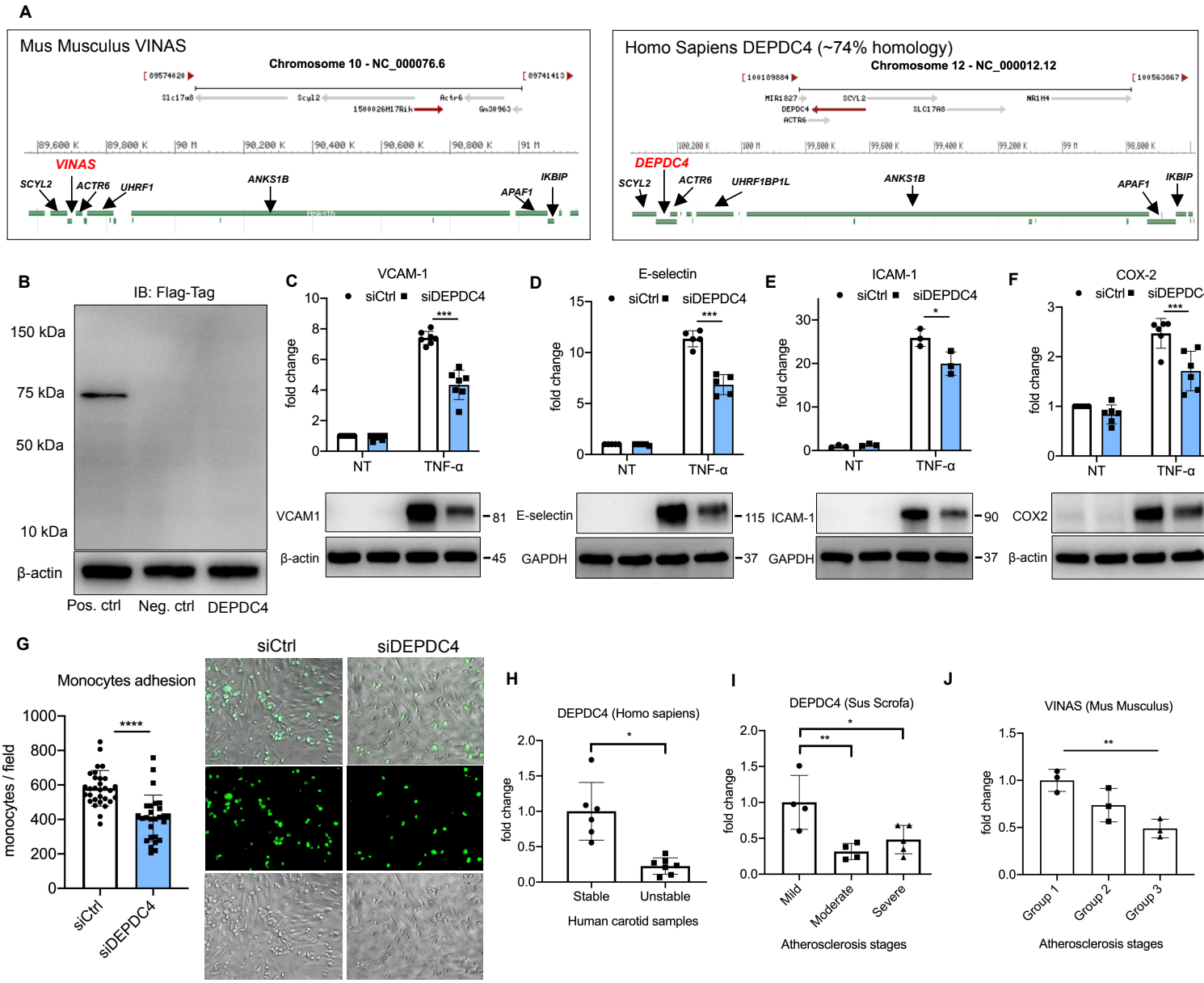
A
Mus Musculus VINAS
Chromosome 10 - NC_000076.6
VINAS
SCYL2
ACTR6
UHRF1
ANKS1B
APAF1
IKBIP
Homo Sapiens DEPDC4 (~74% homology)
Chromosome 12 - NC_000012.12
DEPDC4
SCYL2
ACTR6
UHRF1BP1L
ANKS1B
APAF1
IKBIP
B
IB: Flag-Tag
150 kDa
75 kDa
50 kDa
10 kDa
β-actin
Pos. ctrl
Neg. ctrl
DEPDC4
C
VCAM-1
siCtrl
siDEPDC4
fold change
NT
TNF-α
VCAM1
β-actin
D
E-selectin
E-selectin
GAPDH
E
ICAM-1
ICAM-1
GAPDH
F
COX-2
COX2
β-actin
G
siCtrl
siDEPDC4
Monocytes adhesion
monocytes / field
H
DEPDC4 (Homo sapiens)
Stable
Unstable
Human carotid samples
I
DEPDC4 (Sus Scrofa)
Mild
Moderate
Severe
Atherosclerosis stages
J
VINAS (Mus Musculus)
Group 1
Group 2
Group 3
Atherosclerosis stages

Fig. 6. DEPDC4 is a human ortholog of VINAS. A. Illustration of the genomic locations of *VINAS* and DEPDC4 in the mouse and human chromosomes 10 and 12, respectively. **B.** DEPDC4 does not encode for a protein or peptide. To test the coding potential, DEPDC4 sequence was cloned upstream of the 3xFlag-Tag cassette, transfected in 293T cells, and immunoblotted for Flag antibody; positive control was provided with the kit (n=3 experiments). DEPDC4 silencing decreases the protein expression of VCAM-1 (**C**; n=7), E-selectin (**D**; n=5), and ICAM-1 (**E**; n=3) COX-2 (**E**; n=6) in HUVECs activated with 20 ng/ml TNF-α. **G.** DEPDC4 knockdown decreases THP-1 monocyte adhesion to HUVEC monolayers activated with TNF-α for 4 hours (5 ng/ml, representative images and quantification of adhered monocytes). **H**. RT-qPCR of DEPDC4 in human carotid arteries with stable (n=6) or unstable (n=7) atherosclerotic plaques; Scale bar, 50 μm. **I**. Expression of DEPDC4 from RNA-Seq analyses of lesions with increasing severity of coronary atherosclerosis in yorkshire pigs fed a high cholesterol diet for 60 weeks (n=4/group). **J.** RT-qPCR of *VINAS* expression in aortic intima of LDLR-/- mice at 0, 2, and 12 weeks of high cholesterol diet (n=3/group). For all panels values are mean ± SD; Statistical differences were calculated using unpaired two-tailed Student's t-test for all panels except for multiple comparisons (I, J) where one-way ANOVA with Bonferroni correction was used. *p<0.05, **p<0.01; ***p<0.001; ****p<0.0001.

Fig. 7

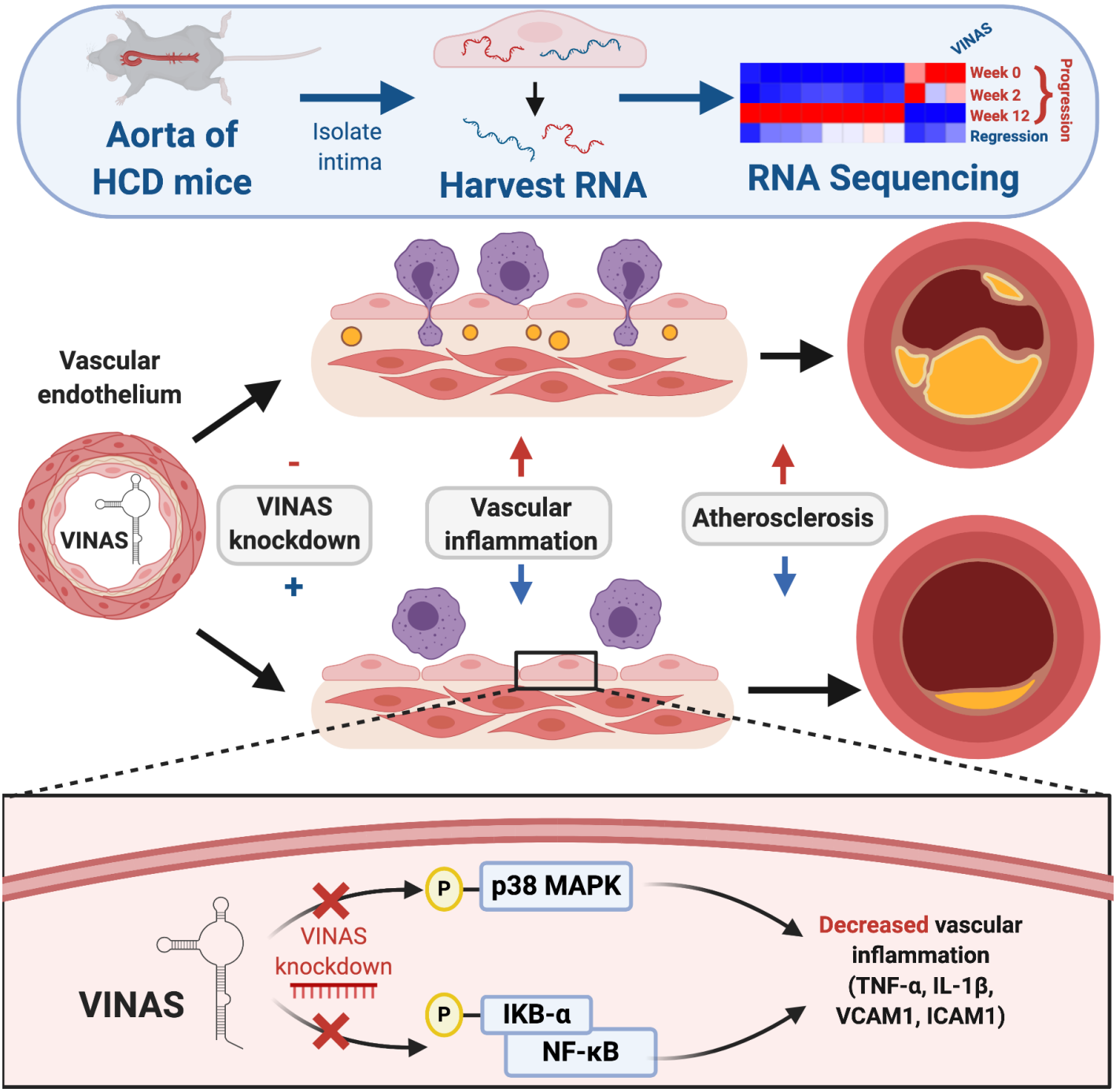
Aorta of HCD mice
Isolate intima
Harvest RNA
VINAS
Week 0
Week 2
Week 12
Regression
Progression
RNA Sequencing
Vascular endothelium
VINAS
-
VINAS knockdown
+
Vascular inflammation
Atherosclerosis
VINAS
VINAS knockdown
P
p38 MAPK
P
IKB-α
NF-κB
Decreased vascular inflammation (TNF-α, IL-1β, VCAM1, ICAM1)

Fig. 7. Graphical Abstract. RNAseq profiling of intimal lesions revealed VINAS lncRNA that is enriched in the aortic intima, decreased with atherosclerotic progression and increased with regression. VINAS knockdown decreased the expression of key inflammatory markers, NF-κB and MAPK signaling pathways, cell adhesion molecules and the monocytes adhesion to ECs. *In vivo* VINAS knockdown reduced atherosclerotic lesion formation in LDLR-/- mice by decreasing vascular inflammation.